

**Protein Structure and Folding:  
Structural Insights into the Substrate  
Specificity of a 6-Phospho-  $\beta$ -glucosidase  
BglA-2 from *Streptococcus pneumoniae*  
TIGR4**



Wei-Li Yu, Yong-Liang Jiang, Andreas Pikis,  
Wang Cheng, Xiao-Hui Bai, Yan-Min Ren,  
John Thompson, Cong-Zhao Zhou and  
Yuxing Chen

*J. Biol. Chem.* 2013, 288:14949-14958.

doi: 10.1074/jbc.M113.454751 originally published online April 11, 2013

---

Access the most updated version of this article at doi: [10.1074/jbc.M113.454751](https://doi.org/10.1074/jbc.M113.454751)

Find articles, minireviews, Reflections and Classics on similar topics on the [JBC Affinity Sites](#).

Alerts:

- [When this article is cited](#)
- [When a correction for this article is posted](#)

[Click here](#) to choose from all of JBC's e-mail alerts

Supplemental material:

<http://www.jbc.org/content/suppl/2013/04/11/M113.454751.DC1.html>

This article cites 42 references, 15 of which can be accessed free at  
<http://www.jbc.org/content/288/21/14949.full.html#ref-list-1>

# Structural Insights into the Substrate Specificity of a 6-Phospho- $\beta$ -glucosidase BglA-2 from *Streptococcus pneumoniae* TIGR4<sup>\*[5]</sup>

Received for publication, January 19, 2013, and in revised form, April 10, 2013. Published, JBC Papers in Press, April 11, 2013, DOI 10.1074/jbc.M113.454751

Wei-Li Yu<sup>‡</sup>, Yong-Liang Jiang<sup>‡</sup>, Andreas Pikis<sup>§¶</sup>, Wang Cheng<sup>‡</sup>, Xiao-Hui Bai<sup>‡</sup>, Yan-Min Ren<sup>‡</sup>, John Thompson<sup>§</sup>, Cong-Zhao Zhou<sup>‡1</sup>, and Yuxing Chen<sup>‡2</sup>

From the <sup>‡</sup>Hefei National Laboratory for Physical Sciences at the Microscale and School of Life Sciences, University of Science and Technology of China, Hefei Anhui 230027, China, the <sup>§</sup>Microbial Biochemistry and Genetics Section, Laboratory of Cell and Developmental Biology, NIDCR, National Institutes of Health, Bethesda, Maryland 20892, and the <sup>¶</sup>Center for Drug Evaluation and Research, Food and Drug Administration, Silver Spring, Maryland 20993

**Background:** *Streptococcus pneumoniae* BglA-2 is a GH-1 6-phospho- $\beta$ -glucosidase with specificity toward 1,4-linked 6-phospho- $\beta$ -glucosides.

**Results:** BglA-2 and other GH-1 members adopt a similar overall structure and catalytic mechanism.

**Conclusion:** Tyr<sup>126</sup>, Tyr<sup>303</sup>, and Trp<sup>338</sup> determine substrate specificity, and Ser<sup>424</sup>, Lys<sup>430</sup>, and Tyr<sup>432</sup> discriminate phosphorylated from non-phosphorylated substrate. A tryptophan residue discriminates 6-phospho- $\beta$ -glucosidase from 6-phospho- $\beta$ -galactosidase activities.

**Significance:** BglA-2 structures provide new insight into characteristics and substrate specificity of 6-phospho- $\beta$ -glucosidase.

The 6-phospho- $\beta$ -glucosidase BglA-2 (EC 3.2.1.86) from glycoside hydrolase family 1 (GH-1) catalyzes the hydrolysis of  $\beta$ -1,4-linked cellobiose 6-phosphate (cellobiose-6'P) to yield glucose and glucose 6-phosphate. Both reaction products are further metabolized by the energy-generating glycolytic pathway. Here, we present the first crystal structures of the apo and complex forms of BglA-2 with thiocellobiose-6'P (a non-metabolizable analog of cellobiose-6'P) at 2.0 and 2.4 Å resolution, respectively. Similar to other GH-1 enzymes, the overall structure of BglA-2 from *Streptococcus pneumoniae* adopts a typical ( $\beta/\alpha$ )<sub>8</sub> TIM-barrel, with the active site located at the center of the convex surface of the  $\beta$ -barrel. Structural analyses, in combination with enzymatic data obtained from site-directed mutant proteins, suggest that three aromatic residues, Tyr<sup>126</sup>, Tyr<sup>303</sup>, and Trp<sup>338</sup>, at subsite +1 of BglA-2 determine substrate specificity with respect to 1,4-linked 6-phospho- $\beta$ -glucosides. Moreover, three additional residues, Ser<sup>424</sup>, Lys<sup>430</sup>, and Tyr<sup>432</sup> of BglA-2, were found to play important roles in the hydrolytic selectivity toward phosphorylated rather than non-phosphorylated compounds. Comparative structural analysis suggests that a tryptophan *versus* a methionine/alanine residue at subsite –1 may contribute to the catalytic and substrate selectivity with

respect to structurally similar 6-phospho- $\beta$ -galactosidases and 6-phospho- $\beta$ -glucosidases assigned to the GH-1 family.

Pathogenic strains of *Streptococcus pneumoniae* are the primary cause of acute pneumonia, otitis media, and meningitis in humans (1–3). During infection and colonization, abundant carbon sources are needed to support growth of the organism in host cells. For this purpose, 32 carbohydrates have been identified as energy sources for *S. pneumoniae*, including three-carbon molecules (glycerol), nine hexoses or hexose derivatives, three  $\alpha$ -galactosides, two  $\beta$ -galactosides, four  $\alpha$ -glucosides, seven  $\beta$ -glucosides, and six polysaccharides (4). In *S. pneumoniae*, the accumulation of carbohydrates is facilitated by three major types of sugar transporters (5, 6), including phosphoenolpyruvate-dependent phosphotransferase system (PEP-PTS)<sup>3</sup> transporters (7–11), cation/proton-coupled transporters (12, 13), and ATP-binding cassette transporters (14–16). Among them, the most ubiquitous PEP-PTS systems in bacteria are responsible for the uptake of various carbohydrates, such as glucose, sucrose, mannitol, fructose, lactose, mannose, and cellobiose (11). During transport via the PEP-PTS, sugars, including the disaccharide cellobiose (Fig. 1), are simultaneously phosphorylated at the C6 hydroxyl moiety during entry into the cell (10). The gene *SP\_0578* encoding a 6-phospho- $\beta$ -glucosidase BglA-2 from *S. pneumoniae* TIGR4 resides in a

<sup>\*</sup> This work was supported, in whole or in part, by the National Institutes of Health, NIDCR, Intramural Research Program. This work was also supported by Ministry of Science and Technology of China Grant 2009CB918800, National Natural Science Foundation of China Grant 31270781, and Research Fund for the Doctoral Program of Higher Education of China Grant 20123402110004.

The atomic coordinates and structure factors (codes 4IPL and 4IPN) have been deposited in the Protein Data Bank (<http://www.pdb.org/>).

[5] This article contains supplemental Tables S1 and S2 and Figs. S1–S3.

<sup>1</sup> To whom correspondence may be addressed. Tel.: 86-551-63602492; Fax: 86-551-63600406; E-mail: cyxing@ustc.edu.cn.

<sup>2</sup> To whom correspondence may be addressed. Tel.: 86-551-63602492; Fax: 86-551-63600406; E-mail: zcz@ustc.edu.cn.

<sup>3</sup> The abbreviations used are: PEP-PTS, phosphoenolpyruvate-dependent phosphotransferase system; PTS, phosphotransferase system; cellobiose-6'P,  $\beta$ -1,4-linked cellobiose 6-phosphate; G6P, glucose 6-phosphate; GH-1, glycoside hydrolase family 1; pNP $\beta$ Glc6P, *p*-nitrophenyl- $\beta$ -D-glucopyranoside 6-phosphate; PMP, 1-phenyl-3-methyl-5-pyrazolone; thiocellobiose-6'P, thiocellobiose 6-phosphate; lactose-6'P, lactose 6-phosphate; galactose-6'P, galactose 6-phosphate; oNP $\beta$ Gal6P, *o*-nitrophenyl- $\beta$ -D-galactopyranoside 6-phosphate; PGALase, 6-phospho- $\beta$ -galactosidase; gentiobiose 6'P,  $\beta$ -1,6-linked glucose 6-phosphate and glucose; maltose-6'P,  $\alpha$ -1,4-linked glucose 6-phosphate and glucose.

### Substrate Specificity of the 6-Phospho- $\beta$ -glucosidase BglA-2

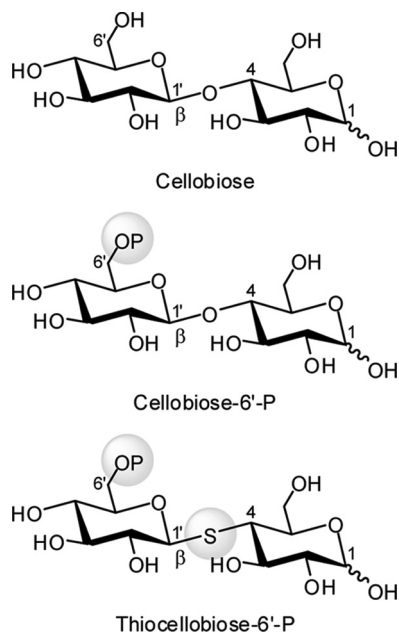


**FIGURE 1. Structural formulas of cellobiose and its derivatives.**

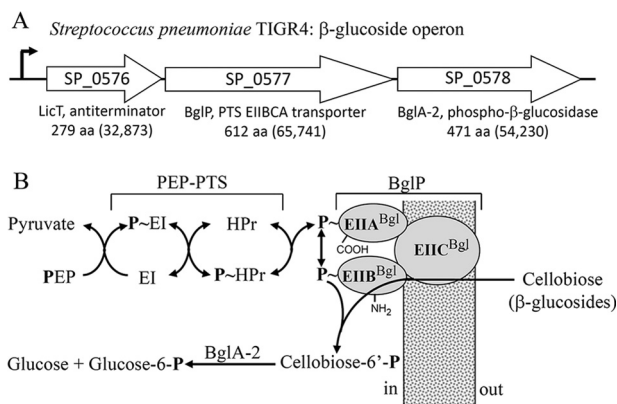


FIGURE 2. *A*, genetic organization of the  $\beta$ -glucoside operon in *S. pneumoniae* TIGR4. SP numbers represent the order of gene loci. Values in parentheses are calculated molecular weights of encoded proteins. *B*, translocation and phosphorylation of cellobiose by the multicomponent  $\beta$ -glucoside PEP-PTS and BglA-2-catalyzed hydrolysis of cellobiose-6'-P.

three-gene operon (Fig. 2A) comprising a transcription anti-terminator *LicT* (*SP\_0576*) and a downstream gene *BglP* (*SP\_0577*) encoding a  $\beta$ -glucoside PEP-PTS transporter. This operon is present in a number of species, including *Streptococcus mutans*, *Clostridium longisporum*, and *Listeria monocytogenes*. BglP comprises three domains, EIIA, EIIB, and EIIC, that facilitate the simultaneous translocation and phosphorylation of cellobiose and related  $\beta$ -glycosides (Fig. 2B). The transmembrane permease domain (EIIC) is responsible for recognition and binding of specific substrates, and the incoming sugars are phosphorylated by EIIA and EIIB domains of the PTS (17, 18). BglA-2 hydrolyzes cellobiose 6'-phosphate (cellobiose-6'P) to yield G6P and glucose (Fig. 2B) that are further metabolized by the energy-generating glycolytic pathway (17, 19). Based on the sequence similarity, BglA-2 is assigned to glycoside hydrolase family 1 (GH-1), which includes a variety of glycoside hydrolases, such as 6-phospho- $\beta$ -glucosidase (EC 3.2.1.86), 6-phospho- $\beta$ -galactosidase (EC 3.2.1.85), and  $\beta$ -glucosidase (EC

3.2.1.21) (20). Members of the GH-1 family share a common catalytic mechanism and exhibit similar structural folds, including a  $(\beta/\alpha)_8$  TIM-barrel. As described in Koshland's double displacement mechanisms (21, 22), two conserved acidic residues (glutamate or aspartate) are catalytic residues. One of these amino acids functions as a proton donor, and the other functions as a nucleophile. First the proton donor provides a proton to the substrate to protonate the glycosidic oxygen, with the attendant formation of the transient oxocarbenium state. Then the nucleophile residue attacks the protonated glycosidic bond and forms a glycosyl-enzyme intermediate. Finally, a water molecule provides a proton to break the glycosyl-enzyme intermediate, thus restoring the enzyme to its original protonated state.

Several structures of GH-1 members are now available (23–26), but (to our knowledge) there are no reports of the co-crystallization of an intact substrate at the active site of any GH-1 phospho- $\beta$ -glucosidase. Significantly, the mechanism and determinants of enzyme specificity toward 1,4-linked 6-phospho- $\beta$ -glucosides remain unclear. In this work, we present the first crystal structures of BglA-2 in both the apo form and in complex with thiocellobiose-6'-P at 2.0 and 2.4 Å, respectively. Structural analysis, in combination with the enzymatic data obtained from site-directed mutants, has enabled us to define the structural elements that contribute to enzyme recognition of 1,4-linked 6-phospho- $\beta$ -glucosides. Importantly, we provide evidence that three key residues, Ser<sup>424</sup>, Lys<sup>430</sup>, and Tyr<sup>432</sup> of BglA-2, play functional roles in enzyme discrimination between the hydrolysis of phosphorylated and the non-phosphorylated substrates. Finally, results obtained via site-directed mutagenesis show that a tryptophan residue plays an important role in substrate discrimination between 6-phospho- $\beta$ -galactosidases and 6-phospho- $\beta$ -glucosidases in the GH-1 family.

## EXPERIMENTAL PROCEDURES

**Cloning, Expression, and Purification of BglA-2 and Its Mutants**—The coding sequence of the *bglA*-2 gene was amplified from the genomic DNA of *S. pneumoniae* TIGR4. The *bglA*-2 gene and its mutants were respectively cloned into the pET28a (Novagen) expression vector with an N-terminal His<sub>6</sub> tag. Both the wild-type and mutant proteins were overexpressed in *Escherichia coli* strain BL21(DE3) (Novagen) using 2× YT culture medium (5 g of NaCl, 16 g of Bacto-Tryptone, and 10 g of yeast extract/liter). The transformed cells were grown at 37 °C in 2× YT medium containing 30 μg/ml kanamycin until the *A*<sub>600 nm</sub> reached 0.6–0.8. Expression of the recombinant proteins was then induced by the addition of 0.2 mM isopropyl β-D-1-thiogalactopyranoside for 20 h at 16 °C. The cells were collected by centrifugation at 8,000 × *g* for 10 min and resuspended in 45 ml of lysis buffer (20 mM Tris-Cl, pH 8.0, 100 mM NaCl). After 6 min of sonication and 30 min of centrifugation at 12,000 × *g*, the supernatant containing the target protein was collected and loaded onto a nickel-nitrilotriacetic acid column (GE Healthcare) equilibrated with the binding buffer (20 mM Tris-Cl, pH 8.0, 100 mM NaCl). The column was washed with binding buffer, and the target protein was then eluted with the same buffer containing 300 mM imidazole. The target protein was then loaded onto a Superdex 200 column



(GE Healthcare), and fractions containing the target protein were collected and pooled. The purified protein was concentrated to 10 mg/ml by ultrafiltration (Amicon, Millipore Corp.) for crystallization trials. Samples for enzymatic activity assays were collected at the highest peak fractions without concentration. The purity of protein was assessed by SDS-PAGE, and the protein sample was stored at  $-80^{\circ}\text{C}$ . Site-directed mutagenesis was performed using the QuikChange site-directed mutagenesis kit (Stratagene, La Jolla, CA) with the plasmid encoding the wild-type BglA-2 serving as template. The mutant proteins were expressed, purified, and stored as described above.

**Crystallization, Data Collection, and Processing**—Both the apo and complex forms of BglA-2 were concentrated to 10 mg/ml by ultrafiltration for crystallization. All crystals were grown at  $16^{\circ}\text{C}$  using the sitting drop vapor diffusion technique. Each drop contained 1  $\mu\text{l}$  of protein sample (10 mg/ml protein in buffer containing 20 mM Tris-Cl, pH 8.0, 100 mM NaCl) with an equal volume of the reservoir solution (15% polyethylene glycol 5000MME, 0.1 M sodium citrate tribasic dehydrate, pH 5.6). The crystals were transferred to cryoprotectant (reservoir solution supplemented with 25% glycerol) and flash-cooled with liquid nitrogen. All diffraction data were collected at 100 K in a liquid nitrogen stream at the Shanghai Synchrotron Radiation Facility. The data were integrated with the program Mosflm (27) and scaled with the program Scala in CCP4i (28).

**Structure Determination and Refinement**—The structure of apo form BglA-2 was solved by molecular replacement with MOLREP using the coordinates of 50% sequence-identical *E. coli* BglA (Protein Data Bank code 2XHY) as the search model. The complex form of BglA-2 (with thiocellobiose-6'P) was solved by molecular replacement using the apo form BglA-2 as the search model. The initial model was further refined by using the maximum likelihood method implemented in REFMAC5 (29) as part of the CCP4i (28) program suite and rebuilt interactively by using the  $\sigma$ A-weighted electron density maps with coefficients  $2F_o - F_c$  and  $F_o - F_c$  in the program COOT (30). The final model was evaluated with the programs MOLPROBITY (31) and PROCHECK (32). The data collection and structure refinement statistics of apo form and complex form BglA-2 are listed in Table 1. All of the structure figures were prepared with the program PyMOL (33).

**Enzymatic Activity Assays**—The kinetic parameters of wild-type BglA-2 and its mutants were determined using chromogenic *p*-nitrophenyl- $\beta$ -D-glucopyranoside 6-phosphate (pNP $\beta$ Glc6P) as substrate (34). All assays were performed at  $37^{\circ}\text{C}$  in a buffer containing 50 mM  $\text{Na}_2\text{HPO}_4$ , 50 mM  $\text{NaH}_2\text{PO}_4$ , pH 7.5, and reactions were initiated by the addition of BglA-2. Changes in absorption at 405 nm (formation of *p*-nitrophenol) were monitored continuously using a DU800 spectrophotometer (Beckman Coulter, Fullerton, CA). The reaction product *p*-nitrophenol was calculated from a standard curve of *p*-nitrophenol, as described by Prag *et al.* (35). Michaelis-Menten parameters ( $V_{\text{max}}$  and  $K_m$ ) of BglA-2 were extracted from these data by nonlinear fitting to the Michaelis-Menten equation using the program Origin version 7.5.

**TABLE 1**  
Crystal parameters, data collection, and structure refinement

	Apo form	Complex form
<b>Data collection</b>		
Space group	C2	C2
Unit cell		
$a, b, c$ ( $\text{\AA}$ )	183.28, 65.35, 126.69	184.03, 66.65, 133.35
$\alpha, \beta, \gamma$ (degrees)	90.00, 133.38, 90.00	90.00, 136.33, 90.00
Resolution range ( $\text{\AA}$ )	42.9–2.0	46.0–2.4
Unique reflections	72,464 (10,190) <sup>a</sup>	42,473 (5,887)
Completeness (%)	98.8 (95.7)	98.2 (94.6)
$\langle I/\sigma(I) \rangle$	8.8 (4.5)	15.3 (6.5)
$R_{\text{merge}}^b$ (%)	8.3 (17.1)	5.1 (11.2)
Average redundancy	3.4 (3.2)	3.5 (3.0)
<b>Structure refinement</b>		
Resolution range ( $\text{\AA}$ )	31.7–2.0	46.0–2.4
$R$ factor <sup>c</sup> / $R$ -free <sup>d</sup> (%)	17.7/22.2	17.5/25.1
No. of protein atoms	7,504	7,522
No. of water atoms	579	202
RMSD <sup>e</sup> bond lengths ( $\text{\AA}$ )	0.007	0.007
RMSD bond angles (degrees)	1.159	1.143
Mean $B$ factors ( $\text{\AA}^2$ )	20.4	44.5
Ramachandran plot <sup>f</sup> (residues, %)		
Most favored (%)	99.2	98.1
Additional allowed (%)	0.8	1.9
Outliers (%)	0	0
Protein Data Bank entry	4IPL	4IPN

<sup>a</sup> The values in parentheses refer to statistics in the highest bin.

<sup>b</sup>  $R_{\text{merge}} = \sum_{hkl} \sum_i |I_i(hkl) - \langle I(hkl) \rangle| / \sum_{hkl} \sum_i I_i(hkl)$ , where  $I_i(hkl)$  is the intensity of an observation, and  $\langle I(hkl) \rangle$  is the mean value for its unique reflection. Summations are over all reflections.

<sup>c</sup>  $R$  factor =  $\sum_h |F_o(h) - F_c(h)| / \sum_h F_o(h)$ , where  $F_o$  and  $F_c$  are the observed and calculated structure factor amplitudes, respectively.

<sup>d</sup>  $R$ -free was calculated with 5% of the data excluded from the refinement.

<sup>e</sup> Root mean square deviation from ideal values.

<sup>f</sup> Categories were defined by Molprobity.

**Preparation of 1-Phenyl-3-methyl-5-pyrazolone (PMP) Derivatives**—PMP derivation of saccharides was performed as described previously (36–38) with minor changes. Briefly, 10  $\mu\text{l}$  of reaction mixture was mixed with 10  $\mu\text{l}$  of 0.3 M aqueous NaOH and 10  $\mu\text{l}$  of 0.5 M methanol solution of PMP. The total reaction mixture (30  $\mu\text{l}$ ) was maintained at  $70^{\circ}\text{C}$  for 30 min, cooled to room temperature, and neutralized by the addition of 10  $\mu\text{l}$  of 0.3 M HCl. The solution was further mixed with 100  $\mu\text{l}$  of chloroform. After vigorous shaking and centrifugation, the organic phase was carefully removed to eliminate excess reagents. The extraction procedure was repeated three times. Finally, the aqueous phase containing derivatives was diluted with 40  $\mu\text{l}$  of water prior to HPLC analysis.

**HPLC Analysis**—The assays with specific substrate were performed at  $37^{\circ}\text{C}$  in a 10- $\mu\text{l}$  system containing the buffer of 50 mM  $\text{Na}_2\text{HPO}_4$ , 50 mM  $\text{NaH}_2\text{PO}_4$ , pH 7.5, and the disaccharide substrate (e.g. cellobiose-6'P) at a range of concentrations. The reactions were initiated by the addition of the purified enzymes and were terminated by the addition of 10  $\mu\text{l}$  of 0.3 M NaOH. After PMP derivation, the reaction product was centrifuged at  $12,000 \times g$  for 10 min, and 15  $\mu\text{l}$  of supernatant was analyzed by an HPLC system (Agilent 1200 series). Glucose and G6P standards were quantified by HPLC analysis using various concentrations ranging from 0.1 to 1 mM. The mixing buffer containing 20% acetonitrile and 100 mM  $\text{Na}_2\text{HPO}_4/\text{NaH}_2\text{PO}_4$ , pH 7.0 was processed as described previously (38) for equilibration of the column (Eclipse XDB-C18 column,  $4.6 \times 150$  mm; Agilent), and separation of the components was effected at a flow rate of 1 ml/min. Retention times of monosaccharides were determined by comparison with standard solutions. Kinetic parameters were derived from three inde-

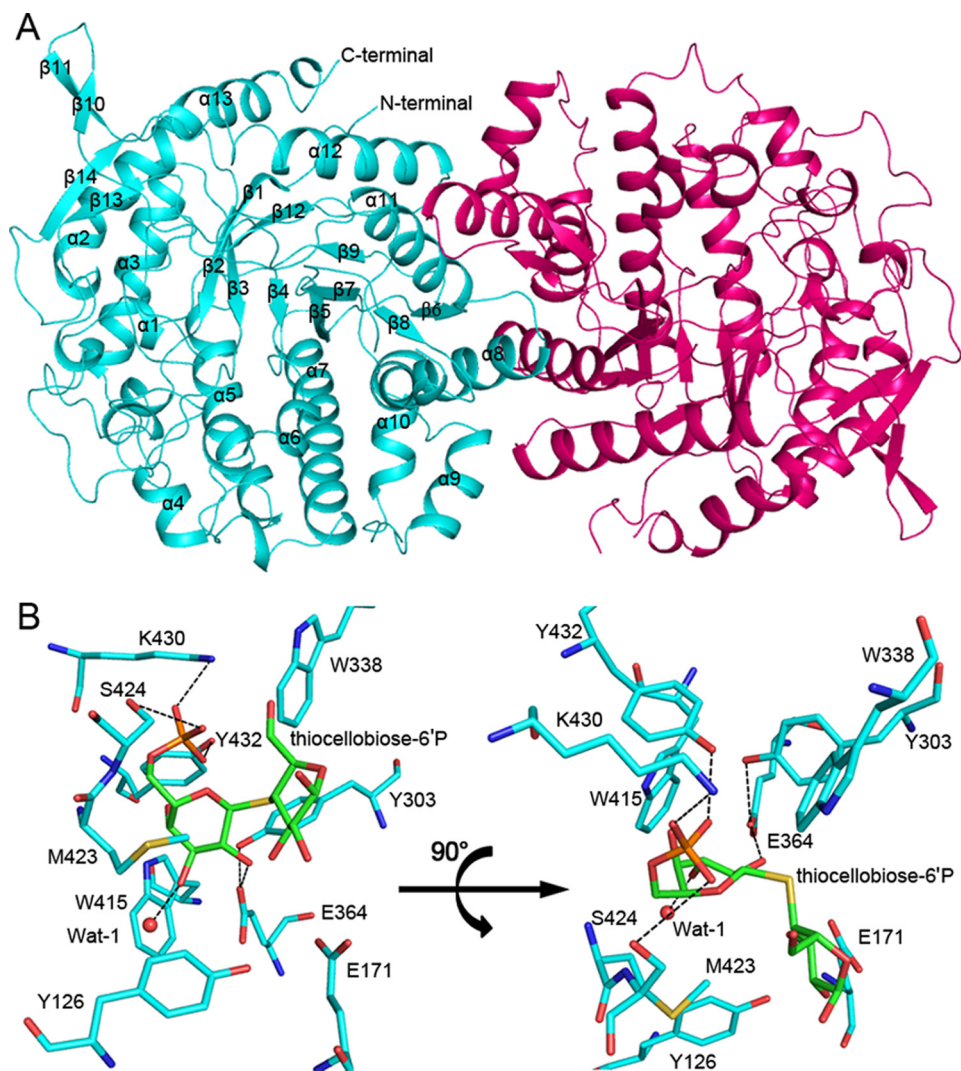


FIGURE 3. **Overall structure and the active site of BglA-2.** A, schematic representation of the overall structure of the dimeric BglA-2 (cyan, subunit A; red, subunit B). The secondary structural elements are labeled. B, the active site of BglA-2 from two angles. The active site residues and the thiocellobiose-6'P are shown as cyan and green sticks for the C $\alpha$  atoms, respectively. A water molecule at the active site is shown as a red sphere. Polar interactions are indicated by dashed lines.

pendent experiments in order to calculate the means and S.D. for the  $K_m$  and  $k_{cat}$  values.

**Preparation of Cellobiose-6'P, Thiocellobiose-6'P, and pNP $\beta$ Glc6P**—Cellobiose was obtained from Pfanstiehl Laboratories, and thiocellobiose was purchased from Toronto Research Chemicals. Phosphorylation of the primary hydroxyl groups of the non-reducing glucose moiety in these O- $\beta$ -linked disaccharides was as described previously (39). In brief, phosphorylation was effected by incubation of the disaccharides with ATP-dependent  $\beta$ -glucoside kinase (BglK, EC 2.7.1.85) from *Klebsiella pneumoniae*. Phosphorylated derivatives were first isolated by Ba<sup>2+</sup> and ethanol precipitation and further purified by ion exchange and paper chromatography. Structures and product purity were confirmed by thin layer chromatography, mass spectrometry, and NMR spectroscopy. Chromogenic pNP $\beta$ Glc6P was prepared by phosphorylation of the C6 hydroxyl moiety of pNP- $\beta$ -D-glucopyranoside with phosphorus oxychloride in trimethyl phosphate containing a small amount of water (34). Lactose-6'-phosphate (lactose-6'P) is not commercially available, and the chromogenic analog o-nitro-

phenyl- $\beta$ -D-galactopyranoside 6-phosphate (oNP $\beta$ Gal6P; Sigma-Aldrich) was used as a substitute substrate for kinetics analyses.

## RESULTS AND DISCUSSION

**Overall Structure**—The crystal structure of apo form BglA-2 was determined at 2.0 Å resolution in the space group C2. Each asymmetric unit contains two molecules, which form a stable dimer with a buried interface area of  $\sim 3,300$  Å<sup>2</sup> (Fig. 3A). The dimerization in the crystal structure is consistent with the results obtained from size exclusion chromatography (supplemental Fig. S1). The dimer interface, composed of four  $\alpha$ -helices ( $\alpha 8$ ,  $\alpha 9$ ,  $\alpha 11$ , and  $\alpha 12$ ) and three loops from one subunit, is stabilized primarily by a number of polar residues via hydrogen bond networks and salt bridge interactions. Similar to other reported GH-1 members, BglA-2 adopts a typical ( $\beta/\alpha$ )<sub>8</sub> TIM-barrel: a central eight-stranded ( $\beta 1$ – $\beta 5$ ,  $\beta 7$ ,  $\beta 9$ , and  $\beta 12$ ) parallel  $\beta$ -sheet surrounded by eight helices ( $\alpha 2$ ,  $\alpha 3$ ,  $\alpha 5$ ,  $\alpha 7$ ,  $\alpha 8$ , and  $\alpha 11$ – $\alpha 13$ ). In addition, the central TIM-barrel is packed by four additional helices ( $\alpha 1$ ,  $\alpha 6$ ,  $\alpha 9$ , and  $\alpha 10$ ) and six  $\beta$ -strands

TABLE 2

Kinetic constants of BglA-2 and mutants toward pNP $\beta$ Glc6P and cellobiose-6'P

Enzyme	pNP $\beta$ Glc6P			Cellobiose-6'P		
	$K_m$	$k_{cat}$	$k_{cat}/K_m \times 10^{-1}$	$K_m$	$k_{cat}$	$k_{cat}/K_m \times 10^{-1}$
	$\mu M$	$s^{-1}$	$s^{-1} \mu M^{-1}$	$\mu M$	$s^{-1}$	$s^{-1} \mu M^{-1}$
Wild type	478 $\pm$ 4.5	195 $\pm$ 5.3	4.1 $\pm$ 0.3	1135 $\pm$ 9.8	170 $\pm$ 3.8	1.5 $\pm$ 0.2
E171A	ND <sup>a</sup>	ND	ND	ND	ND	ND
E171Q	ND	ND	ND	ND	ND	ND
E364A	ND	ND	ND	ND	ND	ND
E364Q	ND	ND	ND	ND	ND	ND
Y126A	ND	ND	ND	ND	ND	ND
Y126F	598 $\pm$ 3.8	146 $\pm$ 6.4	2.4 $\pm$ 0.2	1515 $\pm$ 11.8	138 $\pm$ 7.8	0.9 $\pm$ 0.1
Y303A	ND	ND	ND	ND	ND	ND
Y303F	ND	ND	ND	ND	ND	ND
W338A	ND	ND	ND	ND	ND	ND
M423A	512 $\pm$ 4.8	168 $\pm$ 8.3	3.3 $\pm$ 0.4	1320 $\pm$ 10.5	145 $\pm$ 8.9	1.1 $\pm$ 0.3
S424A	ND	ND	ND	ND	ND	ND
K430A	ND	ND	ND	ND	ND	ND
Y432F	ND	ND	ND	ND	ND	ND

<sup>a</sup> ND, no detectable activity.

( $\beta$ 6,  $\beta$ 8,  $\beta$ 10,  $\beta$ 11,  $\beta$ 13, and  $\beta$ 14). Residues Asn<sup>316</sup>–Gly<sup>324</sup> in both the apo form and complex form are rather flexible and are absent in the final model due to the poor electron density. A molecule of thiocellobiose-6'P is bound at the center of the TIM-barrel in the complex structure. Structural comparison of the apo and complex structures revealed similar conformations, with a root mean square deviation of 0.3 Å over 436 Ca atoms.

To date, the crystal structures of four 6-phospho- $\beta$ -glycosidases from the GH-1 family have been solved, including three 6-phospho- $\beta$ -glucosidases (*E. coli* BglA, *S. mutans* putative 6-phospho- $\beta$ -glucosidase Bgl, and *Lactobacillus plantarum* Pbg1) and one 6-phospho- $\beta$ -galactosidase (PGALase) from *Lactococcus lactis*. These proteins assume a structure similar to that of BglA-2 with an overall root mean square deviation of 2.0, 1.2, 1.3, and 1.4 Å, respectively. The main differences reside in the architecture surrounding the active site pockets. In the complex structure of PGALase with galactose 6-phosphate (galactose-6'P), three antiparallel  $\beta$ -strands and an 11-residue loop (Gln<sup>305</sup>–Arg<sup>334</sup>) cover the catalytic pocket, whereas in BglA-2, the corresponding region (Asn<sup>316</sup>–Gly<sup>324</sup>) is absent from the structure. In BglA, the loop (Asp<sup>38</sup>–Pro<sup>62</sup>) caps the entrance of the substrate tunnel, whereas in BglA-2, the corresponding loop (Leu<sup>36</sup>–Leu<sup>52</sup>) is considerably shorter. Despite a similar catalytic mechanism, the variable loops around the active sites may reflect the substrate specificity of each enzyme, which is in agreement with the variety of substrates hydrolyzed by GH-1 members.

**The Active Site**—As is evident from the BglA-2 complex structure, thiocellobiose-6'P is stabilized at the active site pocket via hydrophilic and hydrophobic interactions (Fig. 3B). In detail, the phosphate group that projects toward the base of the pocket is hydrogen-bonded by the side chains of Ser<sup>424</sup>, Lys<sup>430</sup>, and Tyr<sup>432</sup>. In subsite –1 G6P is anchored by hydrophobic interaction with Trp<sup>415</sup> and is also hydrogen-bonded to one of the catalytic residues (Glu<sup>364</sup>) and a water molecule, Wat-1. The side chain of the catalytic residue Glu<sup>171</sup> resides ~6 Å from the glycosidic bond. Subsite +1 is occupied by glucose and includes three aromatic residues: Tyr<sup>126</sup>, Tyr<sup>303</sup>, and Trp<sup>338</sup>. In addition, Tyr<sup>303</sup> makes a hydrogen bond with the carboxyl group of Glu<sup>364</sup>, presumably to orient and maintain Glu<sup>364</sup> in a conformation favorable for catalysis.

When compared with the representative complex structure of PGALase with galactose-6'P in the GH-1 family, many of the active site residues of BglA-2 can be superimposed, especially the two catalytic residues Glu<sup>364</sup> and Glu<sup>171</sup> (corresponding to Glu<sup>375</sup> and Glu<sup>160</sup> of PGALase and Glu<sup>375</sup> and Glu<sup>176</sup> of Bgl) (23). Notably, the distances between the side chains of PGALase Glu<sup>160</sup> and Bgl Glu<sup>176</sup> and the glycosidic bond are 3.4 and 2.8 Å, respectively, which are favorable for catalysis. Structural comparison of BglA-2 with PGALase and Bgl reveals that the thiocellobiose-6'P adopts a similar position but different conformation. Thus, our structure might be a complex for the interactions of thiocellobiose-6'P with BglA-2 that is not poised for catalysis.

These observations suggest that BglA-2 adopts a catalytic mechanism similar to those of previously documented GH-1 members (21, 22). The fact that mutant proteins E364A, E364Q, E171A, and E171Q lose all catalytic activity toward pNP $\beta$ Glc6P and cellobiose-6'P confirms the crucial roles of Glu<sup>364</sup> and Glu<sup>171</sup> in BglA-2 catalysis (Table 2).

**Key Residues Contributing to Specificity at Subsite +1**—GH-1 enzymes with known structures are reported to specifically catalyze the hydrolysis of 1,4-linked non-phosphorylated  $\beta$ -glycosides or 1,4-linked 6-phospho- $\beta$ -glycosides.  $\beta$ -Glucosidase A from *Bacillus polymyxa* reportedly hydrolyzes  $\beta$ -1,4-linked oligosaccharides composed of more than 2 units of glucose (25), and human cytosolic  $\beta$ -glucosidase hydrolyzes certain flavonoid glucosides (26). The enzyme PGALase from *L. lactis* was reported to hydrolyze lactose-6'P, formed during transport and phosphorylation via the lactose PEP-PTS (23). The model of lactose-6'P bound to PGALase predicted that Trp<sup>347</sup> at the channel entrance and Tyr<sup>299</sup> and Trp<sup>421</sup> at the substrate cavity were involved in guiding and binding the substrate by hydrophobic interactions (24). Compared with BglA-2, Trp<sup>421</sup> of PGALase corresponds to subsite –1 Trp<sup>415</sup>, whereas Tyr<sup>299</sup> and Trp<sup>347</sup> of PGALase are aligned with subsite +1 Tyr<sup>303</sup> and Trp<sup>338</sup>, respectively. Although the structures of  $\beta$ -glucosidase A, cytosolic  $\beta$ -glucosidase, and PGALase are known, a lack of enzymatic assays and 6-phospho- $\beta$ -glucoside complexed structure leaves the substrate specificity of 6-phospho- $\beta$ -glucosidases still ambiguous. To address the structural basis of the substrate specificity toward 1,4-linked 6-phospho- $\beta$ -glucosides, concerted efforts were made to obtain crystals of



BglA-2 in complex with cellobiose-6'P, pNP $\beta$ Glc6P, glucose, G6P, and thiocellobiose-6'P. Fortuitously, phospho- $\beta$ -glucosidases in family GH-1 are unable to hydrolyze this phosphorylated cellobiose analog. (By contrast, phospho- $\beta$ -glucosidases assigned to family GH-4 readily cleave thiocellobiose-6'P by a catalytically unique series of oxidation-elimination-addition and reduction reactions (40, 41).) After numerous attempts, the structure of BglA-2 in complex with thiocellobiose-6'P was successfully solved. Inspection of the complex shows that the hexose ring at the subsite +1 moiety is orientated almost perpendicular to that of the G6P in subsite -1. The glucose moiety at subsite +1 is sandwiched by residues Tyr<sup>303</sup> and Trp<sup>338</sup> on one side and on the opposite side by Tyr<sup>126</sup> (Fig. 3B). Among the three subsite +1 residues, Tyr<sup>126</sup> is newly identified in our structure and corresponds to Phe<sup>137</sup> in PGALase. Multiple-sequence alignment among 6-phospho- $\beta$ -glycosidases in the GH-1 family shows that Tyr<sup>126</sup>, Tyr<sup>303</sup>, and Trp<sup>338</sup> are generally conserved in bacteria, besides the only protozoa, *Leishmania infantum* (Fig. 4). To clarify the roles of Tyr<sup>126</sup>, Tyr<sup>303</sup>, and Trp<sup>338</sup> in BglA-2 catalysis, we first determined the equilibrium dissociation constants ( $K_d$ ) of both wild-type and mutant proteins of BglA-2 (Y126A, Y303A, Y303F, and W338A) toward cellobiose-6'P by fluorescence spectrometry. The  $K_d$  values of mutants increased ~6–7-fold compared with the wild type (supplemental Table S1), suggesting that the mutants had much lower cellobiose-6'P binding affinities compared with the wild type. Subsequently, we compared the enzymatic activities of these mutants with that of the wild type. The mutant Y126A was devoid of all activity, whereas Y126F retained ~59% of that of the wild type, indicative of the important role of Tyr<sup>126</sup> in this hydrophobic pocket. Neither the mutant Y303A nor Y303F showed any enzymatic activity (Table 2). These results show that Tyr<sup>303</sup> is essential for activity, not only by contributing to the hydrophobicity of the pocket but also by stabilizing the orientation of the catalytically functional carboxyl group of Glu<sup>364</sup>. This result is in accordance with the complex structure, in which Tyr<sup>303</sup> makes a hydrogen bond with the carboxyl group of Glu<sup>364</sup> (Fig. 3B). The mutant W338A was also completely inactive.

To further study the subsite +1 specificity, we investigated the activity of the wild type and mutants of BglA-2 toward two stereoisomers of cellobiose-6'P, namely gentiobiose-6'P ( $\beta$ -1,6-linked glucose 6-phosphate and glucose) and maltose-6'P ( $\alpha$ -1,4-linked glucose 6-phosphate and glucose). Neither wild-type nor mutant proteins hydrolyzed gentiobiose-6'P or maltose-6'P (supplemental Fig. S2). These results established the specificity of BglA-2 toward cellobiose-6'P. Furthermore, it is evident that the active site residues Tyr<sup>126</sup>, Tyr<sup>303</sup>, and Trp<sup>338</sup> play important roles not only in substrate binding but also in recognition of the unique spatial orientation of glucose (in cellobiose-6'P) that permits this moiety to occupy subsite +1 of BglA-2.

**Key Residues That Dictate Specificity toward the Phosphate Group of Cellobiose-6'P**—As described previously, the phosphate-binding residues Ser<sup>428</sup>, Lys<sup>435</sup>, and Tyr<sup>437</sup> in PGALase discriminate the phosphorylated from the non-phosphorylated sugar (24). In BglA-2, three residues (Ser<sup>424</sup>, Lys<sup>430</sup>, and Tyr<sup>432</sup>) make hydrogen bonds with the phosphate group of thiocello-

biose-6'P (Fig. 3B). Comparison of the complex structures of BglA-2 and PGALase shows that residues Lys<sup>430</sup> and Tyr<sup>432</sup> of BglA-2 adopt a position similar to Lys<sup>435</sup> and Tyr<sup>437</sup> of PGALase, respectively. However, Ser<sup>424</sup> of BglA-2 corresponds to Ser<sup>430</sup> rather than Ser<sup>428</sup> of PGALase. Sequence analysis suggested that Lys<sup>430</sup> and Tyr<sup>432</sup> of BglA-2 are conserved in GH-1 6-phospho- $\beta$ -glycosidases (Fig. 4). However, they are substituted by non-polar residues in other GH-1 glycosidases hydrolyzing non-phosphorylated substrates, such as  $\beta$ -glucosidase A from *B. polymyxa* (25). Indeed, BglA-2 shows no hydrolytic activity toward non-phosphorylated cellobiose. To verify the roles of the three residues, we measured the enzymatic activities toward cellobiose-6'P through use of several mutants. The results showed that mutations S424A, K430A, and Y432F abolished all activity, thereby confirming the key roles of Ser<sup>424</sup>, Lys<sup>430</sup>, and Tyr<sup>432</sup> of BglA-2 in determining specificity toward phosphorylated substrate (Table 2).

Sequence alignment of 6-phospho- $\beta$ -glycosidases in the GH-1 family indicates that two catalytic residues (Glu<sup>364</sup> and Glu<sup>171</sup>); the subsite +1 residues Tyr<sup>126</sup>, Tyr<sup>303</sup>, and Trp<sup>338</sup>; and the phosphate-binding residues Lys<sup>430</sup> and Tyr<sup>432</sup> are exclusively conserved. The observations suggest that these homologs might adopt a similar overall structure and hydrolyze phosphorylated substrates (Fig. 4). Our structural analyses provide new insight into the substrate binding patterns and determinants of specificity of GH-1 family phospho- $\beta$ -glycosidases.

**A Tryptophan Residue Discriminates 6-Phospho- $\beta$ -galactosidase from 6-Phospho- $\beta$ -glucosidase in GH-1 Family**—In GH-1 family, two types of enzymes can hydrolyze phosphorylated substrates. 6-Phospho- $\beta$ -glucosidase and 6-phospho- $\beta$ -galactosidase are distinguished by their subsite -1 sugars, with G6P for 6-phospho- $\beta$ -glucosidase and galactose-6'P for 6-phospho- $\beta$ -galactosidase. Whereas BglA-2 hydrolyzes cellobiose-6'P, PGALase hydrolyzes lactose-6'P. The major difference between cellobiose-6'P and lactose-6'P resides in the orientation of the C4 hydroxyl group of the hexose-6P compounds at subsite -1. In the case of cellobiose-6'P, the equatorial C4 hydroxyl lies on the opposite side of the C1 hydroxyl, whereas in lactose-6'P, the axial C4 hydroxyl moiety lies on the same side as the C1 hydroxyl group. In BglA-2, the subsite -1 sugar (G6P) shifts 2.4 Å apart and rotates about 67° from that of Gal6P in PGALase. This difference between the substrates is in accordance with the active site conformations. In PGALase, the C4 hydroxyl moiety is hydrogen-bonded by Trp<sup>429</sup> (24), which is substituted by Met<sup>423</sup> in BglA-2 or Ala<sup>431</sup> in Bgl (Fig. 5, A and B). However, Met<sup>423</sup> in BglA-2 and Ala<sup>431</sup> in Bgl have no interaction with the subsite -1 sugar. Indeed, no residue was found to stabilize the C4 hydroxyl group of BglA-2 and Bgl. The M423A and M423W mutants of BglA-2 retain about 80 and 67% of the activity of the wild-type enzyme respectively, suggesting a non-essential role for Met<sup>423</sup> in catalysis (Table 2 and supplemental Table S2). In further studies, the activities of the wild-type BglA-2 and M423W mutant were determined using oNP $\beta$ Gal6P as a chromogenic substitute for lactose-6'P. As expected, the wild-type BglA-2 has no detectable activity toward oNP $\beta$ Gal6P. Remarkably, the single mutation M423W elicited hydrolytic activity toward oNP $\beta$ Gal6P with a  $k_{\text{cat}}/K_m$  value of  $8.6 \pm 2.1 \times 10^{-5} \text{ s}^{-1} \mu\text{M}^{-1}$  (supplemental Table S2).



# Substrate Specificity of the 6-Phospho- $\beta$ -glucosidase BglA-2

		TT		$\beta$ 1	$\alpha$ 1	$\eta$ 1	TT		TT	TT		$\alpha$ 2
<i>S. pneumoniae</i>	1	.....	MTIFPDD	FW	GGATAAA	NQVEGAYNEDGKGLSVQ	DVLPKGGGLGEATENP	TEDNKLKI	GTDFYHKYKE	DISEF	SEM	FN
<i>Listeria</i>	1	.....	MHTNTGFPAN	FW	GGAAAA	NQFEAGAYNVGDKGLSVQ	DVLPKGGFGHITDGP	TPDNKLKE	GTDFYHKYKE	DISEF	SEM	FN
<i>Leishmania</i>	1	.....	MSSKFPDH	FW	GGATAA	NQVEGAYQTDGKGLST	DVLPQGFIFGAIVPRVDGSDGKIDV	ADTFYHKYKE	DISEF	SEM	FN	GK
<i>Corynebacterium</i>	1	.....	MSLSHENQSAFFPKD	FW	GGATAA	NQIEGAYNEGGKGLSIQ	DVLPQGLLAPFTKEP	TDDNKLKN	ADTFYHKYKE	DISEF	SEM	FN
<i>Lachnospiraceae</i>	1	.....	MFPKN	FW	GGATAA	NQCEGAYLEDGKGLDIQ	DVTPKGIIVGPRTVEP	TEDNMKLK	ADTFYHKYKE	DISEF	SEM	FN
<i>E. coli</i>	1	.....	MKAFFPET	FW	GGATAA	NQCEGAWQEDGKGLST	DLPQGHVGMKMEPRILGKENIKDV	ADTFYHKYKE	DISEF	SEM	FN	GK
<i>Salmonella</i>	1	.....	MLT	GGAHGV	.....	REITQNVVAGKYYPN	.....	HE	ADTFYHKYKE	DISEF	SEM	FN
<i>Lactococcus</i>	1	.....	MTKTLPKD	FW	GGATAA	YQAEGATHTDGKGPVAV	DKYLE	DNYWYTAEP	ASDFYHKYKE	DISEF	SEM	FN
<i>Seibaldella</i>	1	.....	MERLPED	FW	GGATAA	FQAEAGVNDGGRGKCYW	DEYLHRAESTFNGDT	.....	ASDFYHKYKE	DISEF	SEM	FN
<i>Coprobacillus</i>	1	.....	MKFPDN	FW	GGATAA	YQCEGSTLKYGKGVAV	DLYL	KEGRFSGDP	ASDFYHKYKE	DISEF	SEM	FN
<i>Melissococcus</i>	1	.....	MKKLPDH	FW	GGATAA	YQCEGSTLTKGKGPVAV	DEFLQ	KQGRFSPDP	ASDFYHKYKE	DISEF	SEM	FN
<i>Eubacterium</i>	1	.....	MKFSDD	FW	GGATAA	YQCEGSTLEYGKGVAV	DFLA	KQGRFKADP	ASDFYHKYKE	DISEF	SEM	FN
<i>Clostridium</i>	1	.....	MKLPKD	FW	GGATAA	YQAEGATKEGKGVAV	DFLE	SQGRFLADP	ASDFYHKYKE	DISEF	SEM	FN

		$\beta$ 2	$\eta$ 2	$\alpha$ 3		$\beta$ 3	$\alpha$ 4	$\eta$ 3	$\alpha$ 5																												
<i>S. pneumoniae</i>	78	VFRSTIAWSRI	PK	GDEE	EPNEAGL	KY	VE	LF	DE	LH	AH	TE	PL	SH	YET	LY	L	ARKYHG	WV	DR	RM	TH	F	Y	KE	F	A	R	T	V	I	E	R	Y	K	D	K
<i>Listeria</i>	81	VFRSTIAWSRI	PK	GDEE	EPNEAGL	KY	VE	LF	DE	LH	AH	TE	PL	SH	YET	LY	L	ARKYHG	WV	DR	RM	TH	F	Y	KE	F	A	R	T	V	I	E	R	Y	K	D	K
<i>Leishmania</i>	80	CLRTSTIAWSRI	PK	GDEE	EPNEAGL	KY	VE	LF	DE	LH	AH	TE	PL	SH	YET	LY	L	ARKYHG	WV	DR	RM	TH	F	Y	KE	F	A	R	T	V	I	E	R	Y	K	D	K
<i>Corynebacterium</i>	85	VFRSTIAWSRI	PK	GDEE	EPNEAGL	KY	VE	LF	DE	LH	AH	TE	PL	SH	YET	LY	L	ARKYHG	WV	DR	RM	TH	F	Y	KE	F	A	R	T	V	I	E	R	Y	K	D	K
<i>Lachnospiraceae</i>	76	VFRSTIAWSRI	PK	GDEE	EPNEAGL	KY	VE	LF	DE	LH	AH	TE	PL	SH	YET	LY	L	ARKYHG	WV	DR	RM	TH	F	Y	KE	F	A	R	T	V	I	E	R	Y	K	D	K
<i>E. coli</i>	79	CLRTSTIAWSRI	PK	GDEE	EPNEAGL	KY	VE	LF	DE	LH	AH	TE	PL	SH	YET	LY	L	ARKYHG	WV	DR	RM	TH	F	Y	KE	F	A	R	T	V	I	E	R	Y	K	D	K
<i>Salmonella</i>	49	CFRTSTIAWSRI	PK	GDEE	EPNEAGL	KY	VE	LF	DE	LH	AH	TE	PL	SH	YET	LY	L	ARKYHG	WV	DR	RM	TH	F	Y	KE	F	A	R	T	V	I	E	R	Y	K	D	K
<i>Lactococcus</i>	70	GIRISTIAWSRI	PK	GDEE	EPNEAGL	KY	VE	LF	DE	LH	AH	TE	PL	SH	YET	LY	L	ARKYHG	WV	DR	RM	TH	F	Y	KE	F	A	R	T	V	I	E	R	Y	K	D	K
<i>Seibaldella</i>	70	GIRISTIAWSRI	PK	GDEE	EPNEAGL	KY	VE	LF	DE	LH	AH	TE	PL	SH	YET	LY	L	ARKYHG	WV	DR	RM	TH	F	Y	KE	F	A	R	T	V	I	E	R	Y	K	D	K
<i>Coprobacillus</i>	68	GIRISTIAWSRI	PK	GDEE	EPNEAGL	KY	VE	LF	DE	LH	AH	TE	PL	SH	YET	LY	L	ARKYHG	WV	DR	RM	TH	F	Y	KE	F	A	R	T	V	I	E	R	Y	K	D	K
<i>Melissococcus</i>	69	SLRLSTIAWSRI	PK	GDEE	EPNEAGL	KY	VE	LF	DE	LH	AH	TE	PL	SH	YET	LY	L	ARKYHG	WV	DR	RM	TH	F	Y	KE	F	A	R	T	V	I	E	R	Y	K	D	K
<i>Eubacterium</i>	68	GIRISTIAWSRI	PK	GDEE	EPNEAGL	KY	VE	LF	DE	LH	AH	TE	PL	SH	YET	LY	L	ARKYHG	WV	DR	RM	TH	F	Y	KE	F	A	R	T	V	I	E	R	Y	K	D	K
<i>Clostridium</i>	68	GIRISTIAWSRI	PK	GDEE	EPNEAGL	KY	VE	LF	DE	LH	AH	TE	PL	SH	YET	LY	L	ARKYHG	WV	DR	RM	TH	F	Y	KE	F	A	R	T	V	I	E	R	Y	K	D	K

		$\beta$ 4	$\eta$ 4	$\alpha$ 6	$\eta$ 5	$\alpha$ 7	$\beta$ 5	$\beta$ 6														
<i>S. pneumoniae</i>	163	VKYWTTFNE	IN	SVLE	LPFT	.....	GGIDIPKENLSKQ	LY	QAI	HHEL	VAS	SL	VT	KI	AREINSEF	KVG	CMV	LAMP	AY	EM	TP	.....
<i>Listeria</i>	166	VKYWTTFNE	IN	SVLE	LPFT	.....	GGIDIPKENLSKQ	LY	QAI	HHEL	VAS	SL	VT	KI	AREINSEF	KVG	CMV	LAMP	AY	EM	TP	.....
<i>Leishmania</i>	165	VKYWTTFNE	IN	SVLE	LPFT	.....	GGIDIPKENLSKQ	LY	QAI	HHEL	VAS	SL	VT	KI	AREINSEF	KVG	CMV	LAMP	AY	EM	TP	.....
<i>Corynebacterium</i>	170	VKYWTTFNE	IN	SVLE	LPFT	.....	GGIDIPKENLSKQ	LY	QAI	HHEL	VAS	SL	VT	KI	AREINSEF	KVG	CMV	LAMP	AY	EM	TP	.....
<i>Lachnospiraceae</i>	161	VKYWTTFNE	IN	SVLE	LPFT	.....	GGIDIPKENLSKQ	LY	QAI	HHEL	VAS	SL	VT	KI	AREINSEF	KVG	CMV	LAMP	AY	EM	TP	.....
<i>E. coli</i>	164	VKYWTTFNE	IN	SVLE	LPFT	.....	GGIDIPKENLSKQ	LY	QAI	HHEL	VAS	SL	VT	KI	AREINSEF	KVG	CMV	LAMP	AY	EM	TP	.....
<i>Salmonella</i>	134	VKYWTTFNE	IN	SVLE	LPFT	.....	GGIDIPKENLSKQ	LY	QAI	HHEL	VAS	SL	VT	KI	AREINSEF	KVG	CMV	LAMP	AY	EM	TP	.....
<i>Lactococcus</i>	152	VKYWTTFNE	IN	SVLE	LPFT	.....	GGIDIPKENLSKQ	LY	QAI	HHEL	VAS	SL	VT	KI	AREINSEF	KVG	CMV	LAMP	AY	EM	TP	.....
<i>Seibaldella</i>	153	VKYWTTFNE	IN	SVLE	LPFT	.....	GGIDIPKENLSKQ	LY	QAI	HHEL	VAS	SL	VT	KI	AREINSEF	KVG	CMV	LAMP	AY	EM	TP	.....
<i>Coprobacillus</i>	151	VKYWTTFNE	IN	SVLE	LPFT	.....	GGIDIPKENLSKQ	LY	QAI	HHEL	VAS	SL	VT	KI	AREINSEF	KVG	CMV	LAMP	AY	EM	TP	.....
<i>Melissococcus</i>	151	VKYWTTFNE	IN	SVLE	LPFT	.....	GGIDIPKENLSKQ	LY	QAI	HHEL	VAS	SL	VT	KI	AREINSEF	KVG	CMV	LAMP	AY	EM	TP	.....
<i>Eubacterium</i>	151	VKYWTTFNE	IN	SVLE	LPFT	.....	GGIDIPKENLSKQ	LY	QAI	HHEL	VAS	SL	VT	KI	AREINSEF	KVG	CMV	LAMP	AY	EM	TP	.....
<i>Clostridium</i>	151	VKYWTTFNE	IN	SVLE	LPFT	.....	GGIDIPKENLSKQ	LY	QAI	HHEL	VAS	SL	VT	KI	AREINSEF	KVG	CMV	LAMP	AY	EM	TP	.....

		$\alpha$ 8	$\alpha$ 9	$\alpha$ 10	$\beta$ 7	$\beta$ 8	$\eta$ 6																														
<i>S. pneumoniae</i>	241	KDVVA	ATH	EYENLN	LYFS	DVHVR	GYPN	YAK	RYFK	.....	ENDI	EF	AAE	AE	LLK	NY	..	TVDF	LS	SY	Y	M	SV	TQ	SAL	PTQ	YN	SGE									
<i>Listeria</i>	244	DDII	AVME	EAERKN	YFS	DVHVR	GYPN	YAK	RYFK	.....	ENDI	EF	AAE	AE	LLK	NY	..	TVDF	LS	SY	Y	M	SV	TQ	SAL	PTQ	YN	SGE									
<i>Leishmania</i>	240	EDVL	KAQ	YETQ	LDAC	FDV	HVR	GYPN	YAK	RYFK	.....	ENDI	EF	AAE	AE	LLK	NY	..	TVDF	LS	SY	Y	M	SV	TQ	SAL	PTQ	YN	SGE								
<i>Corynebacterium</i>	248	ADAL	KAQ	YETQ	LDAC	FDV	HVR	GYPN	YAK	RYFK	.....	ENDI	EF	AAE	AE	LLK	NY	..	TVDF	LS	SY	Y	M	SV	TQ	SAL	PTQ	YN	SGE								
<i>Lachnospiraceae</i>	239	DDML	EVME	ERRHM	NDF	LDV	HVR	GYPN	YAK	RYFK	.....	ENDI	EF	AAE	AE	LLK	NY	..	TVDF	LS	SY	Y	M	SV	TQ	SAL	PTQ	YN	SGE								
<i>E. coli</i>	239	QDM	LAEME	ENRRM	MF	FDV	HVR	GYPN	YAK	RYFK	.....	ENDI	EF	AAE	AE	LLK	NY	..	TVDF	LS	SY	Y	M	SV	TQ	SAL	PTQ	YN	SGE								
<i>Salmonella</i>	217	EDVM	FAQ	ESMR	ERY	VFT	DV	YQL	GY	PS	V	NE	W	E	..	RRG	FI	Q	TF	AP	E	DE	EL	KH	..	TVDF	LS	SY	Y	M	SV	TQ	SAL	PTQ	YN	SGE	
<i>Lactococcus</i>	231	DVRA	AE	ED	I	THN	KFL	DV	YQL	GY	PS	V	NE	W	E	..	RRG	FI	Q	TF	AP	E	DE	EL	KH	..	TVDF	LS	SY	Y	M	SV	TQ	SAL	PTQ	YN	SGE
<i>Seibaldella</i>	231	DIRA	AE	ED	I	THN	KFL	DV	YQL	GY	PS	V	NE	W	E	..	RRG	FI	Q	TF	AP	E	DE	EL	KH	..	TVDF	LS	SY	Y	M	SV	TQ	SAL	PTQ	YN	SGE
<i>Coprobacillus</i>	229	DYQA	AE	ED	I	THN	KFL	DV	YQL	GY	PS	V	NE	W	E	..	RRG	FI	Q	TF	AP	E	DE	EL	KH	..	TVDF	LS	SY	Y	M	SV	TQ	SAL	PTQ	YN	SGE
<i>Melissococcus</i>	229	DYQA	AE	ED	I	THN	KFL	DV	YQL	GY	PS	V	NE	W	E	..	RRG	FI	Q	TF	AP	E	DE	EL	KH	..	TVDF	LS	SY	Y	M	SV	TQ	SAL	PTQ	YN	SGE
<i>Eubacterium</i>	230	DYQA	AE	ED	I	THN	KFL	DV	YQL	GY	PS	V	NE	W	E	..	RRG	FI	Q	TF	AP	E	DE	EL	KH	..	TVDF	LS	SY	Y	M	SV	TQ	SAL	PTQ	YN	SGE
<i>Clostridium</i>	229	DYQA	AE	ED	I	THN	KFL	DV	YQL	GY	PS	V	NE	W	E	..	RRG	FI	Q	TF	AP	E	DE	EL	KH	..	TVDF	LS	SY	Y	M	SV	TQ	SAL	PTQ	YN	SGE

		TT	TT	$\alpha$ 11		$\beta$ 9	$\beta$ 10	TT	$\beta$ 11																													
<i>S. pneumoniae</i>	320	GNIIGGLV	N	.....	PY	LE	SE	EW	GO	IT	PI	GR	RI	IL	N	Y	Y	D	R	Y	Q	..	TP	LF	IV	EN	GL	GA	KD	QL	KD	..	ELNN	IL	TV	QD	Y	
<i>Listeria</i>	322	GNIIGGLV	N	.....	PY	LE	SE	EW	GO	IT	PI	GR	RI	IL	N	Y	Y	D	R	Y	Q	..	TP	LF	IV	EN	GL	GA	KD	QL	KD	..	ELNN	IL	TV	QD	Y	
<i>Leishmania</i>	318	ANILNMVP	N	.....	PH	LE	SE	EW	GO	IT	PI	GR	RI	IL	N	Y	Y	D	R	Y	Q	..	TP	LF	IV	EN	GL	GA	KD	QL	KD	..	ELNN	IL	TV	QD	Y	
<i>Corynebacterium</i>	326	GNIIGGLV	N	.....	PH	LE	SE	EW	GO	IT	PI	GR	RI	IL	N	Y	Y	D	R	Y	Q	..	TP	LF	IV	EN	GL	GA	KD	QL	KD	..	ELNN	IL	TV	QD	Y	
<i>Lachnospiraceae</i>	317	GNIIGGLV	N	.....	PH	LE	SE	EW	GO	IT	PI	GR	RI	IL	N	Y	Y	D	R	Y	Q	..	TP	LF	IV	EN	GL	GA	KD	QL	KD	..	ELNN	IL	TV	QD	Y	
<i>E. coli</i>	317	GNIIGGLV	N	.....	PH	LE	SE	EW	GO	IT	PI	GR	RI	IL	N	Y	Y	D	R	Y	Q	..	TP	LF	IV	EN	GL	GA	KD	QL	KD	..	ELNN	IL	TV	QD	Y	
<i>Salmonella</i>	296	G	F	E	G	S	V	P	N	.....	PY	LE	SE	EW	GO	IT	PI	GR	RI	IL	N	Y	Y	D	R	Y	Q	..	TP	LF	IV	EN	GL	GA	KD	QL	KD	Y
<i>Lactococcus</i>	316	NGTGKGS	SK	Y	Q	I	K	G	V	G	R	R	V	A	P	D	Y	P	T	D	D																	



## Substrate Specificity of the 6-Phospho- $\beta$ -glucosidase BglA-2

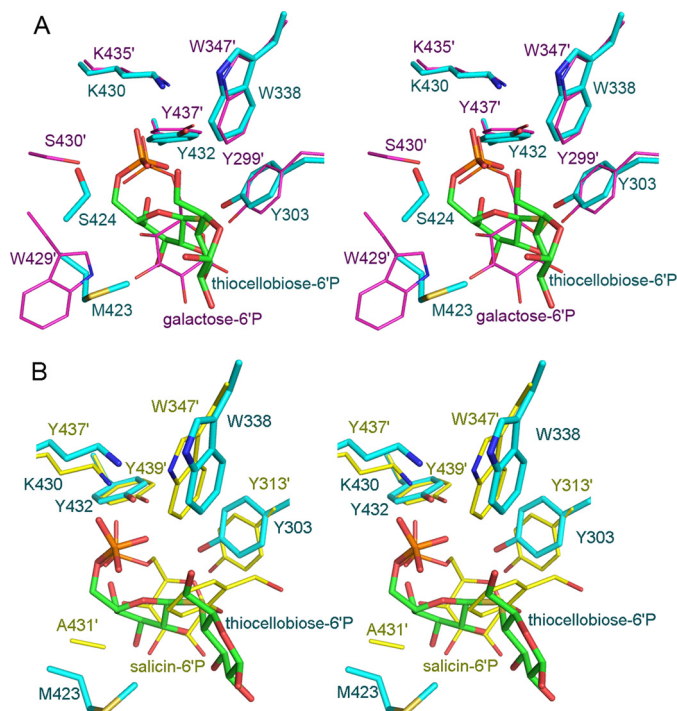


FIGURE 5. Stereo representation of active site comparison of BglA-2 (cyan) with *L. lactis* PGALase (pink; Protein Data Bank code 4PBG) (A) and *S. mutans* Bgl (yellow; Protein Data Bank code 4F79) (B).

These results show that a tryptophan residue of PGALase determines that subsite  $-1$  of this 6-phospho- $\beta$ -galactosidase is occupied by galactose-6'P.

Sequence analysis revealed an  $\sim 50\%$  sequence homology between these two types of enzymes, suggesting a similar structural fold of a  $(\beta/\alpha)_8$  TIM-barrel and a common catalytic mechanism (Fig. 4). However, Trp<sup>429</sup> of PGALase is exclusively conserved in 6-phospho- $\beta$ -galactosidases but is usually alanine in 6-phospho- $\beta$ -glucosidases (Fig. 4). We hypothesize that both enzyme species evolved from a common ancestor, but at some point 6-phospho- $\beta$ -galactosidases evolved independently, such that a tryptophan residue was acquired in order to accommodate galactose-6'P (rather than G6P) at the active site of subsite  $-1$ .

**6-Phospho- $\beta$ -glycosidases Provide Alternative (but Non-essential) Pathways for the Utilization of  $\beta$ -Linked Disaccharides—**Multiple-sequence alignment among 6-phospho- $\beta$ -glycosidases in GH-1 family shows that they are generally conserved in bacteria, with only the protozoa *L. infantum* as the exception (Fig. 4). Abundant bacterial growth is dependent upon the uptake of various carbohydrates from the environment. As noted previously, there are several pathways for the uptake of carbohydrates in bacterial species, including PEP-PTS transporters (7–11), cation/proton-coupled transporters (12, 13), and ATP-binding cassette transporters (14–16). Among these, the group translocation PEP-PTS system is perhaps the most ubiquitous. Many species possess operons that encode genes

for a glycosidase and the appropriate PEP-PTS (4). The PEP-PTS system enables organisms such as *S. pneumoniae* to obtain their metabolic energy via the simultaneous transport and phosphorylation of disaccharides. Intracellular 6-phospho- $\beta$ -glycosidases hydrolyze these phosphorylated compounds to metabolizable monosaccharides that furnish the requisite energy for growth of microorganisms. With the exception of *L. infantum*, 6-phospho- $\beta$ -glycosidases exist only in bacteria, and it is likely that BglA-2 and other 6-phospho- $\beta$ -glycosidases in the GH-1 family have evolved in bacteria simultaneously with the PEP-PTS to permit the dissimilation of environmental disaccharides. The exceptional case of *L. infantum* may be the result of gene transfer from bacteria, as reported previously (42).

Inspection of the 2.16-megabase genome of *S. pneumoniae* TIGR4 reveals three PEP-PTS systems (SP\_0303-10, SP\_0577, and SP\_2021-4), and a sugar efflux transporter that may participate in the utilization and metabolism of cellobiose by this organism (4, 5, 43). For the PEP-PTS systems, cellobiose should be phosphorylated to cellobiose-6'P prior to hydrolysis by 6-phospho- $\beta$ -glucosidases, such as BglA-2 of the SP\_0577 PTS operon and SP\_0303 of the SP\_0303-10 PTS operon. Alternatively, cellobiose may be transported into the cell via a sugar efflux transporter and hydrolyzed intracellularly by putative cellobiase(s) encoded by SP\_2021 and SP\_0265. As reported previously (4), growth of *S. pneumoniae* on cellobiose is essentially abolished upon deletion of the transporter gene SP\_0310 of the SP\_0303-10 PTS, suggesting that this PEP-PTS may be essential for the uptake of cellobiose. By contrast, the  $\Delta$ SP\_0577 strain shows a doubled generation time (195 min) and a prolonged lag period compared with the wild-type strain on methyl- $\beta$ -glucoside, suggesting that SP\_0577 PTS is responsible for the uptake of this and related  $\beta$ -glucosides (4, 18).

Each of the three PEP-PTS systems has a cellobiose/cellobiose-6'P hydrolase that is encoded by the SP\_0303, BglA-2, and SP\_2021 gene, respectively. Structure-based sequence alignment confirms that SP\_0303 and BglA-2 are 6-phospho- $\beta$ -glucosidases, whereas SP\_2021 is most likely a cellobiase. To test whether SP\_0303 and/or BglA-2 are essential for the utilization of cellobiose, we constructed  $\Delta$ BglA-2 and  $\Delta$ BglA-2: $\Delta$ SP\_0303 strains and recorded the growth profiles. The results showed no significant difference of growth rate on cellobiose between the wild-type and deletion strains (supplemental Fig. S3). Although a functional 6-phospho- $\beta$ -glucosidase may not be essential for the utilization of cellobiose, 6-phospho- $\beta$ -glycosidases encoded by PEP-PTS systems provide *S. pneumoniae* with alternate pathways for dissimilation of this carbohydrate and other  $\beta$ -linked disaccharides.

In summary, we have solved the crystal structure of BglA-2 in complex with the non-metabolizable analog, thiocellobiose-6'P. Based on structural analysis and enzymatic assays, we have clarified issues pertaining to the architectural environments of subsites  $-1$  and  $+1$  and have identified residues that interact

FIGURE 4. Multiple-sequence alignment of BglA-2 and homologs. The 6-phospho- $\beta$ -glucosidases and 6-phospho- $\beta$ -galactosidases are labeled with red and black titles, respectively. Two conserved catalytic glutamate residues and the subsite  $-1$  residue Trp<sup>415</sup> are depicted by green triangles. The subsite  $+1$  residues and the phosphate-binding residues are marked with red and black triangles, respectively. The tryptophan residue discriminating 6-phospho- $\beta$ -galactosidase from 6-phospho- $\beta$ -glucosidase in GH-1 family is indicated by a blue triangle.

with the phosphate moiety of G6P at subsite -1 of 6-phospho- $\beta$ -glucosidase. Importantly, we present evidence that a tryptophan residue plays a functional role in the differentiation of the catalytic properties of 6-phospho- $\beta$ -galactosidases and those of 6-phospho- $\beta$ -glucosidases assigned to GH-1 of the glycoside hydrolase family.

**Acknowledgments**—We thank the staff at the Shanghai Synchrotron Radiation Facility for expert technical assistance. We also appreciate the efforts of Kang Zhou with data collection and thank the developers of the CCP4 Suite, ESPript, TreeView, and PyMOL programs. We thank Drs. Josef Deutscher and Stefan Immel for assistance in compiling Figs. 1 and 2.

## REFERENCES

- Kadioglu, A., Weiser, J. N., Paton, J. C., and Andrew, P. W. (2008) The role of *Streptococcus pneumoniae* virulence factors in host respiratory colonization and disease. *Nat. Rev. Microbiol.* **6**, 288–301
- Cartwright, K. (2002) Pneumococcal disease in western Europe. Burden of disease, antibiotic resistance and management. *Eur. J. Pediatr.* **161**, 188–195
- Steinfurt, C., Wilson, R., and Mitchell, T. (1989) Effects of *Streptococcus pneumoniae* on human respiratory epithelium *in vitro*. *Infect. Immun.* **57**, 2006–2013
- Bidossi, A., Mulas, L., Decorosi, F., Colomba, L., Ricci, S., Pozzi, G., Deutscher, J., Viti, C., and Oggioni, M. R. (2012) A functional genomics approach to establish the complement of carbohydrate transporters in *Streptococcus pneumoniae*. *PLoS One* **7**, e33320
- Saier, M. H., Jr. (2000) Families of transmembrane sugar transport proteins. *Mol. Microbiol.* **35**, 699–710
- Ajdić, D., and Pham, V. T. (2007) Global transcriptional analysis of *Streptococcus mutans* sugar transporters using microarrays. *J. Bacteriol.* **189**, 5049–5059
- Kundig, W., Ghosh, S., and Roseman, S. (1964) Phosphate bound to histidine in a protein as an intermediate in a novel phosphotransferase system. *Proc. Natl. Acad. Sci. U.S.A.* **52**, 1067–1074
- Reizer, J., Saier, M. H., Jr., Deutscher, J., Grenier, F., Thompson, J., and Hengstenberg, W. (1988) The phosphoenolpyruvate:sugar phosphotransferase system in gram-positive bacteria. Properties, mechanism, and regulation. *Crit. Rev. Microbiol.* **15**, 297–338
- Roseman, S. (1989) Sialic acid, serendipity, and sugar transport. Discovery of the bacterial phosphotransferase system. *FEMS Microbiol. Rev.* **5**, 3–11
- Meadow, N. D., Fox, D. K., and Roseman, S. (1990) The bacterial phosphoenol-pyruvate. Glycose phosphotransferase system. *Annu. Rev. Biochem.* **59**, 497–542
- Postma, P. W., Lengeler, J. W., and Jacobson, G. R. (1993) Phosphoenolpyruvate:carbohydrate phosphotransferase systems of bacteria. *Microbiol. Rev.* **57**, 543–594
- Henderson, P. J., Baldwin, S. A., Cairns, M. T., Charalambous, B. M., Dent, H. C., Gunn, F., Liang, W. J., Lucas, V. A., Martin, G. E., and McDonald, T. P. (1992) Sugar-cation symport systems in bacteria. *Int. Rev. Cytol.* **137**, 149–208
- Poolman, B., Knol, J., van der Does, C., Henderson, P. J., Liang, W. J., Leblanc, G., Pourcher, T., and Mus-Veteau, I. (1996) Cation and sugar selectivity determinants in a novel family of transport proteins. *Mol. Microbiol.* **19**, 911–922
- Davidson, A. L. (2002) Mechanism of coupling of transport to hydrolysis in bacterial ATP-binding cassette transporters. *J. Bacteriol.* **184**, 1225–1233
- Davidson, A. L., and Chen, J. (2004) ATP-binding cassette transporters in bacteria. *Annu. Rev. Biochem.* **73**, 241–268
- Patzlaff, J. S., van der Heide, T., and Poolman, B. (2003) The ATP/substrate stoichiometry of the ATP-binding cassette (ABC) transporter OpuA. *J. Biol. Chem.* **278**, 29546–29551
- Thompson, J., Pikis, A., Ruvinov, S. B., Henrissat, B., Yamamoto, H., and Sekiguchi, J. (1998) The gene *glvA* of *Bacillus subtilis* 168 encodes a metal-requiring, NAD(H)-dependent 6-phospho- $\alpha$ -glucosidase. Assignment to family 4 of the glycosylhydrolase superfamily. *J. Biol. Chem.* **273**, 27347–27356
- Cote, C. K., Cvitkovitch, D., Bleiweis, A. S., Honeyman, A. L. (2000) A novel  $\beta$ -glucoside-specific PTS locus from *Streptococcus mutans* that is not inhibited by glucose. *Microbiology* **146**, 1555–1563
- Tettelin, H., Nelson, K. E., Paulsen, I. T., Eisen, J. A., Read, T. D., Peterson, S., Heidelberg, J., DeBoy, R. T., Haft, D. H., Dodson, R. J., Durkin, A. S., Gwinn, M., Kolonay, J. F., Nelson, W. C., Peterson, J. D., Umayam, L. A., White, O., Salzberg, S. L., Lewis, M. R., Radune, D., Holtzapple, E., Khouri, H., Wolf, A. M., Utterback, T. R., Hansen, C. L., McDonald, L. A., Feldblyum, T. V., Angiuoli, S., Dickinson, T., Hickey, E. K., Holt, I. E., Loftus, B. J., Yang, F., Smith, H. O., Venter, J. C., Dougherty, B. A., Morrison, D. A., Hollingshead, S. K., and Fraser, C. M. (2001) Complete genome sequence of a virulent isolate of *Streptococcus pneumoniae*. *Science* **293**, 498–506
- Henrissat, B. (1991) A classification of glycosyl hydrolases based on amino acid sequence similarities. *Biochem. J.* **280**, 309–316
- Koshland, D. E. (1953) Stereochemistry and the mechanism of enzymic reactions. *Biol. Rev. Camb. Philos. Soc.* **28**, 416–436
- Henrissat, B., Callebaut, I., Fabrega, S., Lehn, P., Mornon, J. P., and Davies, G. (1995) Conserved catalytic machinery and the prediction of a common fold for several families of glycosyl hydrolases. *Proc. Natl. Acad. Sci. U.S.A.* **92**, 7090–7094
- Wiesmann, C., Beste, G., Hengstenberg, W., and Schulz, G. E. (1995) The three-dimensional structure of 6-phospho- $\beta$ -galactosidase from *Lactococcus lactis*. *Structure* **3**, 961–968
- Wiesmann, C., Hengstenberg, W., and Schulz, G. E. (1997) Crystal structures and mechanism of 6-phospho- $\beta$ -galactosidase from *Lactococcus lactis*. *J. Mol. Biol.* **269**, 851–860
- Sanz-Aparicio, J., Hermoso, J. A., Martínez-Ripoli, M., Lequerica, J. L., and Polaina, J. (1998) Crystal structure of  $\beta$ -glucosidase A from *Bacillus polymyxa*. Insights into the catalytic activity in family 1 glycosyl hydrolases. *J. Mol. Biol.* **275**, 491–502
- Tribolo, S., Berrin, J. G., Kroon, P. A., Czjzek, M., and Juge, N. (2007) The crystal structure of human cytosolic  $\beta$ -glucosidase unravels the substrate aglycone specificity of a family 1 glycoside hydrolase. *J. Mol. Biol.* **370**, 964–975
- Leslie, A. G. (1999) Integration of macromolecular diffraction data. *Acta Crystallogr. D Biol. Crystallogr.* **55**, 1696–1702
- Collaborative Computational Project, Number 4 (1994) The CCP4 suite. Programs for protein crystallography. *Acta Crystallogr. D Biol. Crystallogr.* **50**, 760–763
- Murshudov, G. N., Vagin, A. A., and Dodson, E. J. (1997) Refinement of macromolecular structures by the maximum-likelihood method. *Acta Crystallogr. D Biol. Crystallogr.* **53**, 240–255
- Emsley, P., and Cowtan, K. (2004) Coot. Model-building tools for molecular graphics. *Acta Crystallogr. D Biol. Crystallogr.* **60**, 2126–2132
- Davis, I. W., Leaver-Fay, A., Chen, V. B., Block, J. N., Kapral, G. J., Wang, X., Murray, L. W., Arendall, W. B., 3rd, Snoeyink, J., Richardson, J. S., and Richardson, D. C. (2007) MolProbity. All-atom contacts and structure validation for proteins and nucleic acids. *Nucleic Acids Res.* **35**, W375–W383
- Laskowski, R. A., Macarthur, M. W., Moss, D. S., and Thornton, J. M. (1993) Procheck. A program to check the stereochemical quality of protein structures. *J. Appl. Crystallogr.* **26**, 283–291
- DeLano, W. (2010) *The PyMol Molecular Graphics System*, version 1.3r1, Schrodinger LLC, New York
- Thompson, J., Robrish, S. A., Bouma, C. L., Freedberg, D. I., and Folk, J. E. (1997) Phospho- $\beta$ -glucosidase from *Fusobacterium mortiferum*. Purification, cloning, and inactivation by 6-phosphoglucono- $\delta$ -lactone. *J. Bacteriol.* **179**, 1636–1645
- Prag, G., Papanikolaou, Y., Tavlas, G., Vorgias, C. E., Petratos, K., and Oppenheim, A. B. (2000) Structures of chitobiase mutants complexed with the substrate Di-N-acetyl-D-glucosamine. The catalytic role of the conserved acidic pair, aspartate 539 and glutamate 540. *J. Mol. Biol.* **300**, 611–617
- Yang, X., Zhao, Y., Wang, Q., Wang, H., and Mei, Q. (2005) Analysis of the



## Substrate Specificity of the 6-Phospho- $\beta$ -glucosidase BglA-2

- monosaccharide components in *Angelica* polysaccharides by high performance liquid chromatography. *Anal. Sci.* **21**, 1177–1180
37. Honda, S., Akao, E., Suzuki, S., Okuda, M., Takehi, K., and Nakamura, J. (1989) High-performance liquid-chromatography of reducing carbohydrates as strongly ultraviolet-absorbing and electrochemically sensitive 1-phenyl-3-methyl-5-pyrazolone derivatives. *Anal. Biochem.* **180**, 351–357
38. Jiang, Y. L., Yu, W. L., Zhang, J. W., Frolet, C., Di Guilmi, A. M., Zhou, C. Z., Vernet, T., and Chen, Y. (2011) Structural basis for the substrate specificity of a novel  $\beta$ -N-acetylhexosaminidase StrH protein from *Streptococcus pneumoniae* R6. *J. Biol. Chem.* **286**, 43004–43012
39. Thompson, J., Lichtenthaler, F. W., Peters, S., and Pikiš, A. (2002)  $\beta$ -Glucoside kinase (BglK) from *Klebsiella pneumoniae*. Purification, properties, and preparative synthesis of 6-phospho- $\beta$ -D-glucosides. *J. Biol. Chem.* **277**, 34310–34321
40. Yip, V. L., Varrot, A., Davies, G. J., Rajan, S. S., Yang, X., Thompson, J., Anderson, W. F., and Withers, S. G. (2004) An unusual mechanism of glycoside hydrolysis involving redox and elimination steps by a Family 4  $\beta$ -glycosidase from *Thermotoga maritima*. *J. Am. Chem. Soc.* **126**, 8354–8355
41. Yip, V. L. Y., and Withers, S. G. (2006) Family 4 glycosidases carry out efficient hydrolysis of thioglycosides by an  $\alpha,\beta$ -elimination mechanism. *Angew. Chem. Int. Ed.* **45**, 1–5
42. Puri, V., Goyal, A., Sankaranarayanan, R., Enright, A. J., and Vaidya, T. (2011) Evolutionary and functional insights into *Leishmania* META1. Evidence for lateral gene transfer and a role for META1 in secretion. *BMC Evol. Biol.* **11**, 334
43. McKessar, S. J., Hakenbeck, R. (2007) The two-component regulatory system TCS08 is involved in cellobiose metabolism of *Streptococcus pneumoniae* R6. *J. Bacteriol.* **189**, 1342–1350

## References

This article cites 42 articles, 15 of which you can access for free at:  
<http://www.jbc.org/content/288/21/14949#BIBL>